

Task-Space Synchronization of Robot Manipulators Driven by Three-Phase Induction Motors

Felipe J. Torres,* Gerardo V. Guerrero,** Carlos D. García,**
Guillermo Valencia,*** Abraham Claudio,** Jesús D. Mina**

*Division of Engineering Campus Irapuato-Salamanca, University of Guanajuato, Guanajuato, 36885
Mexico (Tel: +52 464 647 9940 ext. 2471; e-mail: fdj.torres@ugto.mx).

**National Technological of Mexico/CENIDET, Morelos, 62490, Mexico

(e-mail: gerardog@cenidet.edu.mx, cgarcia@cenidet.edu.mx, peabraha@cenidet.edu.mx, jmina@cenidet.edu.mx)

*** National Technological of Mexico/Technological Institute of Hermosillo, Sonora, 83170
Mexico (e-mail: gvalencia@ith.mx)

Abstract: This paper investigates the use of the 3-phase induction motor as actuator for driving the task space synchronization of robot manipulators. The dynamic models of the induction motor and robot manipulator are combined to set up a single system called IM-Robot. A Lyapunov-based control law is designed to synchronize the end-effector pose of the master IM-Robot system with the end-effectors pose of the slave IM-Robot system while track a desired trajectory. The controller guarantees global exponential task space synchronization. Performance indices are used to prove that the slave IM-Robot systems synchronize with the master IM-Robot system before tracking the desired trajectory. Simulations results are presented to demonstrate the effectiveness of the proposed approach in comparison with similar control.

Keywords: Synchronization, induction motors, nonlinear systems, robotic manipulators, Lyapunov function.

1. INTRODUCTION

In the industrial production, processes require to execute actions that a single robot can't do it, whereby two or more robots have to synchronize to achieve the assignment. Thus, synchronization is understood like the mechanism to make two or more dynamic systems that developing separately, one of them named master or leader and another slave or follower, concur in a common trajectory from certain time to onwards.

In particular, the most of the control algorithms to achieve synchronization of robot manipulators have been developed in the joint space. Thus, in (Rodríguez-Angeles and Nijmeijer., 2004; Bondhus et al., 2005), robot manipulators are synchronized by means of feedback control with only measurement of the robots' position. In (Chung and Slotine, 2009), based on contraction approach, robots track a common trajectory while yield a formation with directed graph interconnection. Undirected graph interconnection is used in (Bouteraa et al., 2011 and Nuño et al., 2013). In (Ihle et al., 2007 and Wang, 2013), passivity is used to solve topics about constant time-delay, whereas time-varying delay is covered in Min et al. (2009), Yu and Antsaklis (2010) and Abdessameud et al. (2013).

Synchronization of robot manipulators in the task space is achieved in (Kyrkjebo and Pettersen, 2008), where a virtual manipulator is used to synchronize slave robot manipulators under a leader-follower scheme with estimation of leader's

velocity. SCARA robots are synchronized in the workspace through a decentralized architecture by means of force control and collision avoidance in (Anton and Anton, 2011). Systems passivity property is used in (Liu and Chopra, 2011) to synchronize heterogeneous robot manipulators with time-varying delay. In Wang, (2013), robot manipulators synchronize without a leader via a directed strongly connected graph to design an adaptable control against parametric uncertainty. In (Aldana et al., 2013), robot manipulators pose is synchronized by means of Jacobians for the robot position and unit-quaternions for orientation. In (Cicek et al., 2014), synchronization is obtained in both the task space and joint space taking into account parametric uncertainty based on the use of a tracking filtered error. In (Cicek and Dasdemir, 2017), the design of a controller in the task space through the output feedback is shown, when only position measurements are available. In (Duan et al., 2019), a distributed tracking controller is developed to synchronize networked manipulators where the followers have only local interaction.

All of these works about synchronization of robot manipulators consider ideal actuators. In the practice, the most of industrial manipulators are driven by electric motors. In particular, permanent magnet brushless DC servo motors (PMBLDC) are employed due to their facility to control the position and tracking a desired trajectory. However, PMBLDC motors are highly cost by the use of rare-earth like neodymium-iron-boron or samarium-cobalt in the permanent magnet production.

Induction motors (IM) are an alternative because they offer low cost of manufacturing and high output torque, though their disadvantage is given by the difficulty to set control to cause of non-linearity. In this sense, researching has been reported on coupling of induction motors and robot manipulators only to track a desired trajectory in the joint space in (Guerrero and Tang, 2001; Hsu and Fu, 2005; De Diniz et al., 2012).

Motivated by the aforementioned limitation about the consideration of ideal actuators and, moreover, moved by the use of the Induction Motors to drive robot manipulators, in this paper, we propose a novel synchronization control approach in the task space based on the direct kinematics of the whole system, which is established by the combination of both the induction motor dynamics and robot manipulator dynamics.

The objective of this paper is to design a synchronization control approach under a master-slave scheme in the task space of robot manipulators driven by induction motors (IM-Robot) such that the end-effector position and orientation $\chi_i \in \mathbb{R}^m$ of the i_{th} slave IM-Robot synchronize with respect to the end-effector position and orientation $\chi_j \in \mathbb{R}^m$ of the master IM-Robot. The outline of the paper is organized as follows. Section 2 expresses the dynamic models of robot manipulator and IM, besides, describes the combination of the dynamics of robot manipulator and IM. Section 3 gives the details of the synchronization controller design in the task space. Section 4 illustrates the simulation results with a master IM-Robot and one slave IM-Robot with the proposed approach in comparison with known results, besides, analyses the performance indices ITSE and ITAE. For last, Section 5 states the conclusions of this work.

2. DYNAMICAL MODEL OF THE WHOLE SYSTEM: ROBOT MANIPULATOR AND INDUCTION MOTOR.

2.1 Robot manipulator model.

Consider p robot manipulators fully actuated with $k = 1, 2, \dots, n$ links. Vectors of the generalized coordinates in the joint space are indicated by $q_i \in \mathbb{R}^n, i = 1, \dots, p$. Using Euler-Lagrange formalism the dynamic model of the i_{th} robot, frictionless, is given by:

$$M_i(q_i)\ddot{q}_i + C_i(q_i, \dot{q}_i)\dot{q}_i + g_i(q_i) = \tau_i \quad i = 1, \dots, p \quad (1)$$

where $M_i(q_i) \in \mathbb{R}^{n \times n}$ is the inertia matrix, $C_i(q_i, \dot{q}_i) \in \mathbb{R}^{n \times n}$ is the Coriolis and centrifugal forces matrix, $g_i(q_i) \in \mathbb{R}^n$ is the gravity forces vector and $\tau_i \in \mathbb{R}^n$ is the input torques vector. This model holds important properties: (Rodríguez-Angeles and Nijmeijer, 2004)

- The inertia matrix $M_i(q_i) \in \mathbb{R}^{n \times n}$ is symmetric positive definite for all $q_i \in \mathbb{R}^n$.

- If matrix $C_i(q_i, \dot{q}_i) \in \mathbb{R}^{n \times n}$ is defined using the Christoffel symbols, then the matrix $[\dot{M}_i(q_i) - 2C_i(q_i, \dot{q}_i)]$ is skew symmetric, such that for all $x \in \mathbb{R}^n$, $x^T [\dot{M}_i(q_i) - 2C_i(q_i, \dot{q}_i)]x = 0$.

2.2 Induction motor model.

The dynamic model and control of induction motor using the equations in a field oriented frame (d, q) is taken of (Marino et al., 2010). This model includes the mechanical and electrical dynamics of the induction motor where the viscous friction effects are neglected.

$$\begin{aligned} \frac{d\omega_m}{dt} &= \mu\lambda_d i_q - \frac{T_L}{J} \\ \frac{d\rho}{dt} &= n_p \omega_m + \alpha L_m \frac{i_q}{\lambda_d} \\ \frac{d\lambda_d}{dt} &= -\alpha\lambda_d + \alpha L_m i_d \\ \frac{di_d}{dt} &= -\gamma i_d + \alpha\beta\lambda_d + n_p \omega_m i_q + \alpha L_m \frac{i_q^2}{\lambda_d} + \frac{1}{\sigma L_s} u_d \\ \frac{di_q}{dt} &= -\gamma i_q - \beta n_p \omega_m \lambda_d - n_p \omega_m i_d - \alpha L_m \frac{i_q i_d}{\lambda_d} + \frac{1}{\sigma L_s} u_q \end{aligned} \quad (2)$$

where ρ is the angle between the flux linkages calculated as

$$\begin{aligned} \text{of the components } \lambda_a \text{ and } \lambda_b, \quad \rho &= \arctan\left(\frac{\lambda_b}{\lambda_a}\right), \quad \alpha = \frac{R_r}{L_r}, \\ \beta &= \frac{L_m}{\sigma L_s L_r}, \quad \mu = \frac{3}{2} n_p \frac{L_m}{J L_r}, \quad \sigma = 1 - \frac{L_m^2}{L_s L_r} \quad \gamma = \frac{R_s L_r^2 + R_r L_m^2}{\sigma L_s L_r^2}. \end{aligned}$$

ω_m is the angular velocity of the rotor in $\frac{rad}{s}$. i_d, i_q are the currents on the d -axis and q -axis, respectively. λ_d denotes the flux linkages on the d -axis. n_p is the number of pair poles, T_L is the load torque in Nm . J is the motor inertia moment, which is a constant. L_m is the mutual inductance, L_s and L_r are stator and rotor self-inductances, computed of $L_{(m,s,r)} = \frac{X_{(m,s,r)}}{2\pi f}$ where $X_{(m,s,r)}$ is the mutual, stator or rotor inductive reactance; f is the nominal frequency in Hz . R_s and R_r are the stator and rotor resistances in Ω .

Letting u_d and u_q the non-linear state feedback control inputs, given by:

$$\begin{pmatrix} u_d \\ u_q \end{pmatrix} = \sigma L_s \begin{pmatrix} -n_p \omega_m i_q - \alpha L_m \frac{i_q^2}{\lambda_d} - \alpha\beta\lambda_d + v_d \\ n_p \beta \omega_m \lambda_d + n_p \omega_m i_d + \alpha L_m \frac{i_d i_q}{\lambda_d} + v_q \end{pmatrix} \quad (3)$$

Substitution of (3) in the induction motor model (2), the closed-loop system is shown as:

$$\begin{aligned} \frac{d\omega_m}{dt} &= \mu\lambda_d i_q - \frac{T_L}{J} \\ \frac{d\rho}{dt} &= n_p \omega_m + \alpha L_m \frac{i_q}{\lambda_d} \\ \frac{d\lambda_d}{dt} &= -\alpha\lambda_d + \alpha L_m i_d \\ \frac{di_d}{dt} &= -\gamma i_d + v_d \\ \frac{di_q}{dt} &= -\gamma i_q + v_q \end{aligned} \quad (4)$$

where v_d and v_q are the new control inputs come from the next proportional-integral (PI) loops:

$$v_d = K_{d1} (\lambda_{d\text{ref}} - \lambda_d) + K_{d2} \int (\lambda_{d\text{ref}} - \lambda_d) dt \quad (5)$$

$$v_q = K_{q1} (T_{\text{ref}} - T) + K_{q2} \int (T_{\text{ref}} - T) dt \quad (6)$$

$$T_{\text{ref}} = K_{q3} (\omega_{\text{ref}} - \omega_m) + K_{q4} \int (\omega_{\text{ref}} - \omega_m) dt \quad (7)$$

where $\lambda_{d\text{ref}}$, T_{ref} and ω_{ref} are the reference values of the rotor flux, torque and angular velocity. K_{d1} , K_{d2} , K_{q1} , K_{q2} , K_{q3} and K_{q4} are the positive constant gains.

2.3 Combination of robot manipulator dynamics and induction motor dynamics.

Considerer the k_{th} joint, $k=1,2,\dots,n$, of each i_{th} robot manipulator, $i=1,\dots,p$, is being directly driven by a induction motor.

The flux linkages amplitude $\lambda_{d,ik}$ is regulated to the constant reference value $\lambda_{d\text{ref},ik}$, consequently the system given in (4) is reduced to:

$$\begin{aligned} J_{ik} \frac{d\omega_{m,ik}}{dt} &= \mu_{ik} J_{ik} \lambda_{d\text{ref},ik} i_{q,ik} - T_{L,ik} \\ \frac{di_{d,ik}}{dt} &= -\gamma_{ik} i_{d,ik} + v_{d,ik} \\ \frac{di_{q,ik}}{dt} &= -\gamma_{ik} i_{q,ik} + v_{q,ik} \end{aligned} \quad (8)$$

Letting $\mathbf{\Omega}_i = [\omega_{m,i1}, \omega_{m,i2}, \dots, \omega_{m,ik}]^T$, $\mathbf{v}_i = [v_{d,ik} \quad v_{q,ik}]^T$,
 $\mathbf{J}_i = \text{diag}[J_{i1}, J_{i2}, \dots, J_{ik}]$, $\mathbf{T}_{L,i} = [T_{L,i1}, T_{L,i2}, \dots, T_{L,ik}]^T$,
 $\mathbf{B}_i = \text{diag}[\mu_{i1} J_{i1}, \mu_{i2} J_{i2}, \dots, \mu_{ik} J_{ik}]$, $\mathbf{I}_i = [i_{d,ik} \quad i_{q,ik}]^T$,
 $\mathbf{\Lambda}_i = [l_{i1}, l_{i2}, \dots, l_{ik}]$ with $l_{ik} = \lambda_{d\text{ref},ik} i_{q,ik}$.

The closed-loop IM reduced model is given by:

$$\begin{aligned} \mathbf{J}_i \dot{\mathbf{\Omega}}_i &= \mathbf{B}_i \mathbf{\Lambda}_i - \mathbf{T}_{L,i} \\ \dot{\mathbf{I}}_i &= -\gamma_{ik} \mathbf{I}_i + \mathbf{v}_i \end{aligned} \quad (9)$$

where $\dot{\mathbf{\Omega}}_i, \mathbf{T}_{L,i}, \mathbf{\Lambda}_i \in \mathbb{R}^n$; $\mathbf{J}_i, \mathbf{B}_i \in \mathbb{R}^{n \times n}$.

Vectors of angular position, velocity and acceleration of the ik_{th} motor are set as $\boldsymbol{\theta}_{m,i}, \boldsymbol{\omega}_{m,i}, \dot{\boldsymbol{\omega}}_{m,i} \in \mathbb{R}^n$.

Assumption 1. There is a direct-drive mechanism between the induction motor and the joint of the robot manipulator, for this reason:

$$\begin{aligned} q_i &= \theta_{m,i} \\ \dot{q}_i &= \omega_{m,i} \\ \ddot{q}_i &= \dot{\omega}_{m,i} \end{aligned} \quad (10)$$

Assumption 2. An input torque is required for each joint of the robot manipulator to achieve a movement; this torque is taken as the load torque applied to the induction motor. Thus,

$$T_{L,i} = \tau_i = M_i \ddot{q}_i + C_i \dot{q}_i + g_i(q_i) \quad (11)$$

Substituting (10) and (11) into (9):

$$\begin{aligned} J_i \dot{\mathbf{\Omega}}_i &= B_i \mathbf{\Lambda}_i - [M_i \ddot{q}_i + C_i \dot{q}_i + g_i(q_i)] \\ B_i \mathbf{\Lambda}_i &= J_i \ddot{q}_i + [M_i \ddot{q}_i + C_i \dot{q}_i + g_i(q_i)] \\ B_i \mathbf{\Lambda}_i &= (J_i + M_i) \ddot{q}_i + C_i \dot{q}_i + g_i(q_i) \\ D_i \ddot{q}_i + C_i \dot{q}_i + g_i(q_i) &= B_i \mathbf{\Lambda}_i \end{aligned} \quad (12)$$

where $D_i = J_i + M_i$.

This whole system IM-Robot from (12) holds the same properties enumerated in Section 2 due to $\dot{D}_i = \dot{J}_i + \dot{M}_i = \dot{M}_i$, J_i is a constant.

Assumption 3. The required torque to attain synchronization is the reference torque T_{ref} in the PI controller of (7).

3. CONTROLLER DESIGN FOR SYNCHRONIZATION IN THE TASK-SPACE

The position and orientation of the end-effector in the task space, denoted by $\chi(t) \in \mathbb{R}^m$, is defined as Behal et al. (2010):

$$\chi = \begin{bmatrix} x(t) \\ y(t) \\ z(t) \end{bmatrix} = f(q) \quad (13)$$

where $f(q) \in \mathbb{R}^m$ indicates the direct kinematics and $q(t) \in \mathbb{R}^n$ means the angular position of the link in the joint space. The relationships between the task space and joint space are given by:

$$\begin{aligned}\dot{\chi} &= J(q)\dot{q} \\ \ddot{\chi} &= \dot{J}(q)\dot{q} + J(q)\ddot{q}\end{aligned}\quad (14)$$

where $\dot{q}(t), \ddot{q}(t) \in \mathbb{R}^n$ express the velocity and acceleration vectors of the link, respectively.

The Jacobean of the manipulator, denoted by $J(q) \in \mathbb{R}^{m \times n}$, is established as:

$$J(q) = \frac{\partial f(q)}{\partial q} \quad (15)$$

The pseudo-inverse of $J(q)$, referred to $J^+(q) \in \mathbb{R}^{n \times m}$, is:

$$J^+ = J^T (J J^T)^{-1} \quad (16)$$

This pseudo-inverse satisfies the equality $J J^+ = I_m$, where $I_m \in \mathbb{R}^{m \times m}$ is an identity matrix. Moreover, the pseudo-inverse obeys the Moore-Penrose conditions.

The position error in the task space $e(t) \in \mathbb{R}^m$, is defined by:

$$e = \chi_d - \chi \quad (17)$$

where $\chi_d \in \mathbb{R}^m$ depicts the desired trajectory in the task space.

Taking the time derivative of the position error and substituting $\dot{\chi}$ of (14):

$$\begin{aligned}\dot{e} &= \dot{\chi}_d - \dot{\chi} \\ &= \dot{\chi}_d - J(q)\dot{q} + \alpha e - \alpha e \\ &= -\alpha e + J \left[J^+ (\dot{\chi}_d + \alpha e) + (I_n - J^+ J) g - \dot{q} \right]\end{aligned}\quad (18)$$

where αe has been added and subtracted to establish the control formulation, $\alpha \in \mathbb{R}^{m \times m}$ is a positive definite diagonal gain matrix. $I_n \in \mathbb{R}^{n \times n}$ is the $n \times n$ identity matrix and $g(t) \in \mathbb{R}^n$ is a signal built according to the control objective.

Based on the structure of (18), a filtered tracking error $r(t) \in \mathbb{R}^n$ is used to reduce the order of the error dynamic equation, $r(t)$ is defined as:

$$r = J^+ (\dot{\chi}_d + \alpha e) + (I_n - J^+ J) g - \dot{q} \quad (19)$$

The position error of the IM-Robot system in the task space is rewritten by the use of $r(t) \in \mathbb{R}^n$ as:

$$\dot{e} = -\alpha e + J r \quad (20)$$

The time derivative of (19) is:

$$\dot{r} = \frac{d}{dt} \left[J^+ (\dot{\chi}_d + \alpha e) + (I_n - J^+ J) g \right] - \ddot{q} \quad (21)$$

Pre-multiplying (21) by the inertia matrix $D(q)$ of the IM-Robot system of (12) and substituting their dynamics, it results:

$$\begin{aligned}D(q)\dot{r} &= D(q) \left\{ \frac{d}{dt} \left[J^+ (\dot{\chi}_d + \alpha e) + (I_n - J^+ J) g \right] - \ddot{q} \right\} \\ &= D(q) \left\{ \frac{d}{dt} \left[J^+ (\dot{\chi}_d + \alpha e) + (I_n - J^+ J) g \right] \right. \\ &\quad \left. - D(q)\ddot{q} \right\} \\ &= D(q) \left\{ \frac{d}{dt} \left[J^+ (\dot{\chi}_d + \alpha e) + (I_n - J^+ J) g \right] \right. \\ &\quad \left. + C(q, \dot{q})\dot{q} + g(q) - B_i \Lambda_i \right\}\end{aligned}\quad (22)$$

To retain the structure of (19), the term $C(q, \dot{q}) \left[J^+ (\dot{\chi}_d + \alpha e) + (I_n - J^+ J) g \right]$ is added and subtracted, therefore the open-loop IM-Robot system dynamics is given by:

$$\begin{aligned}D(q)\dot{r} &= D(q) \left\{ \frac{d}{dt} \left[J^+ (\dot{\chi}_d + \alpha e) + (I_n - J^+ J) g \right] \right. \\ &\quad \left. + C(q, \dot{q})\dot{q} + g(q) - B_i \Lambda_i \right. \\ &\quad \left. + C(q, \dot{q}) \left[J^+ (\dot{\chi}_d + \alpha e) + (I_n - J^+ J) g \right] \right. \\ &\quad \left. - C(q, \dot{q}) \left[J^+ (\dot{\chi}_d + \alpha e) + (I_n - J^+ J) g \right] \right\} \\ D(q)\dot{r} &= -C(q, \dot{q})r + Y\varnothing - B_i \Lambda_i\end{aligned}\quad (23)$$

The regression matrix/parameters vector $Y\varnothing$, is defined by:

$$\begin{aligned}Y\varnothing &= D(q) \frac{d}{dt} \left\{ J^+ (\dot{\chi}_d + \alpha e) + (I_n - J^+ J) g \right\} \\ &\quad + C(q, \dot{q}) \left\{ J^+ (\dot{\chi}_d + \alpha e) + (I_n - J^+ J) g \right\} + g(q)\end{aligned}\quad (24)$$

where $Y(\ddot{\chi}_d, \dot{\chi}_d, \chi, q, \dot{q}, g, \dot{g}) \in \mathbb{R}^{n \times r}$ is the regression matrix and $\varnothing \in \mathbb{R}^r$ means the constant parameters of the system.

The Lyapunov function proposed is:

$$V(r, e) = \sum_{i=1}^p \left\{ \frac{1}{2} r^T D r + \frac{1}{2} e^T e \right\} \quad (25)$$

The matrix $V(r, e)$ is positive definite for all r, e . $V(r, e) = 0$ if and only if $r = 0, e = 0$; $V(r, e) \rightarrow \infty$ if $r \rightarrow \infty$ and $e \rightarrow \infty$.

The time derivative of $V(r, e)$ results:

$$\dot{V}(r, e) = \sum_{i=1}^p \left\{ r^T \dot{D} r + \frac{1}{2} r^T \dot{D} r + e^T \dot{e} \right\}.$$

By the scalars property, $e^T J r = r^T J^T e$. Furthermore, substituting (22) and (20) into $\dot{V}(r, e)$:

$$\begin{aligned} \dot{V}(r, e) &= \sum_{i=1}^p \left\{ \begin{array}{l} r^T (-Cr + Y\varnothing - B_i\Lambda_i) \\ + \frac{1}{2} r^T \dot{D}r + e^T (-\alpha e + Jr) \end{array} \right\} \\ &= \sum_{i=1}^p \left\{ \begin{array}{l} r^T \left(\frac{1}{2} \dot{D} - C \right) r - e^T \alpha e \\ + r^T (Y\varnothing - B_i\Lambda_i + J^T e) \end{array} \right\} \end{aligned}$$

Applying the skew symmetric property of the matrix $(\dot{D} - 2C)$:

$$\dot{V}(r, e) = -\sum_{i=1}^p \left\{ -e^T \alpha e + r^T (Y\varnothing - B_i\Lambda_i + J^T e) \right\} \quad (26)$$

To force that $\dot{V}(r, e) < 0$, the equality is established:

$$Y\varnothing - B_i\Lambda_i + J^T e = -Kr \quad (27)$$

Substitution of (27) into (26):

$$\dot{V}(r, e) = -\sum_{i=1}^p \left\{ e^T \alpha e + r^T Kr \right\} < 0 \quad (28)$$

Therefore, the error e is global asymptotically stable, in according to (Behal et al., 2010).

From (27), the control law to achieve master-slave synchronization of IM-Robot systems in the task space is given as:

$$B_i\Lambda_i = Y\varnothing + Kr + J^T e \quad (29)$$

where $K \in \mathbb{R}^{n \times n}$ is a positive definite constant gain matrix.

4.1 Control objectives

Consider a master robot manipulator j fully actuated by induction motors to track a desired trajectory in the task space, expressed by:

$$\lim_{t \rightarrow \infty} (\mathcal{X}_{d,k} - \mathcal{X}_{j,k}) = 0 \quad (30)$$

where $\mathcal{X}_{d,k} \in \mathbb{R}^m$ means the desired trajectory in the task space, $\mathcal{X}_{j,k} \in \mathbb{R}^m$ denotes the trajectory of the master IM-Robot.

Besides, multiple slave robot manipulators $i = 1, 2, \dots, n$ fully actuated by induction motors synchronize with respect to the master IM-Robot while track the desired trajectory.

$$\lim_{t \rightarrow \infty} (\mathcal{X}_{j,k} - \mathcal{X}_{i,k}) = 0 \quad (31)$$

The IM-Robots controlled through the control law of (29), for which $g(t) \in \mathbb{R}^n$ is a signal established in according to the control objective. Thus, for the master IM-Robot:

$$g_j(t) = q_d - q_j \quad (32)$$

In relation to slave IM-Robots,

$$g_i(t) = q_i - [q_d + K_{op}(q_i - q_j)] \quad (33)$$

where $K_{op} \in \mathbb{R}^{n \times n}$ indicates a positive definite constant gain matrix.

4. RESULTS

The accomplishment of the proposed synchronization approach is displayed as a result of simulation of robot manipulators type SCARA with $k = 1, 2, 3, 4$ joints actuated by 3-phase induction motors.

To verify the efficiency of the suggested synchronization approach, we deploy a master-slave arrangement to get comparison, which is given by one master IM-Robot j and two slave IM-Robots $i = 1, 2$, at this manner:

- The slave IM-Robot $i1$ is set to achieve synchronization by means of the control law for the robot manipulator given in (Cicek et al., 2014).
- The slave IM-Robot $i2$ is configured to synchronize through the control law (29), proposed in this study.
- In according to the assumption 2 and 3, these torques are considered like the reference torques for the induction motor controls, respectively.

The parameters of the robot manipulators are taken from the datasheet of the BOSCH®-SR8, shown in Table 1. About the induction motors, the necessary data are given in Table 2. Optimal characteristics are considered, where the voltage sources supply the required levels.

Table 1. Parameters of the SCARA BOSH®-SR8 robot

Parameter	Value	Parameter	Value	Parameter	Value
l_1	0.43 m	m_1	15 kg	I_1	0.01542 m_1
l_2	0.37 m	m_2	12 kg	I_2	0.01142 m_2
l_{c1}	0.215 m	m_3	3 kg	$I_3 = I_4$	0.03358 m_3
l_{c2}	0.185 m	m_4	3 kg	g	9.81 m/s^2

Table 2. Parameters of the induction motors

Parameter	Value	Parameter	Value
Power	200 W	Poles	4
Velocity	1732 rpm	Voltage	220V-3 phase
R_s	1.77 Ω	R_r	1.34 Ω
L_{ts}	0.024 H	L_m	0.245 H
L_{tr}	0.013 H	J	0.025 $kg \cdot m^2$

The nominal frequency for each induction motor is set as $f_k = [0.8 \ 0.7 \ 0.6 \ 0.5]^T \text{ Hz}$, from this, the nominal angular velocity are $N_k = [24 \ 21 \ 18 \ 15]^T \text{ rpm}$.

The flux linkage reference for the induction motors is $\lambda_{dref,k} = 0.4 \text{ Wb}$. The gains are set as: $K_{d1} = \text{diag}[2000]$, $K_{d2} = \text{diag}[8000]$, $K_{q3} = \text{diag}[50]$, $K_{q4} = \text{diag}[150]$, $\alpha = \text{diag}[250]$, $K = \text{diag}[30]$ and $K_{op} = \text{diag}[4]$.

The simulation is conducted in Simulink® with the S-Function level 2 codification.

The desired trajectory is depicted by the expression:

$$\chi_d(t) = [0.55 + 0.1 \sin(2t), 0.3 + 0.1 \cos(2t), 0.08t]^T \text{ m} \quad (34)$$

The initial position of the end effector in the task space for the master IM-Robot is set to:

$$\chi(0)_j = [0.37 \ 0.43 \ 0]^T \text{ m} \quad (35)$$

For the slave IM-Robots, the initial position in the task space is given by:

$$\chi(0)_{i=1,2} = [0.2953 \ 0.4235 \ 0]^T \text{ m} \quad (36)$$

Note, subindex $i1$ is used for the slave IM-Robot with control law given in (Cicek et al., 2014); subindex $i2$ is used for the suggested synchronization approach; while subindex j is used for the master IM-Robot.

The synchronization of IM-Robots in the task space on the $x-y$ plane is described in Fig. 1. In Fig. 2, the synchronization is seen from the $x-z$ plane.

The synchronization errors by each axis are shown in Fig. 3, Fig. 4 and Fig. 5. This plots show that synchronization errors converge to zero as time goes to infinity; furthermore, the slave IM-Robots achieve synchronization with the master IM-Robot before to track the desired trajectory.

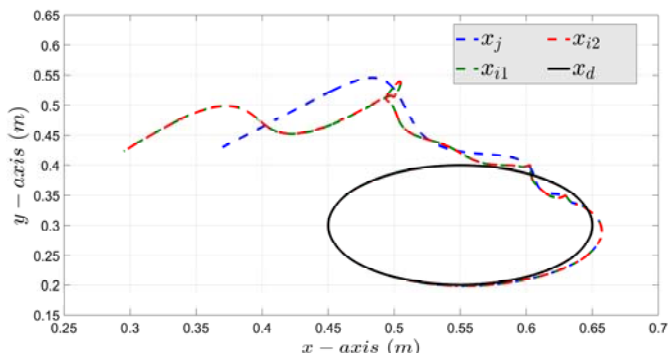


Fig. 1. Synchronization of IM-Robot systems in the task space on the x-y plane.

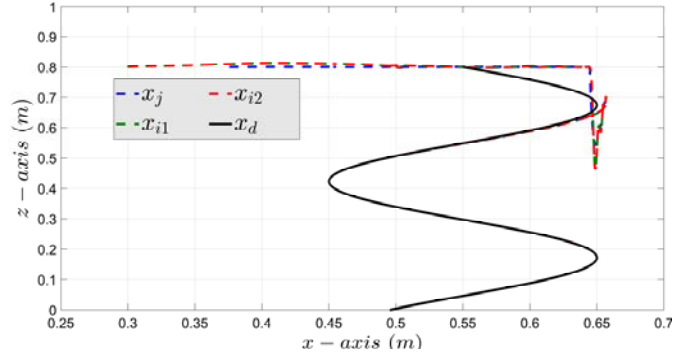


Fig. 2. Synchronization of IM-Robot systems in the task space on the x-z plane.

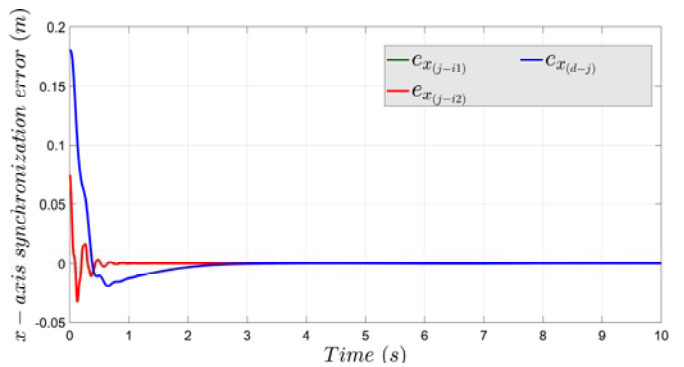


Fig. 3. Synchronization error on the x-axis of IM-Robot systems in the task space.

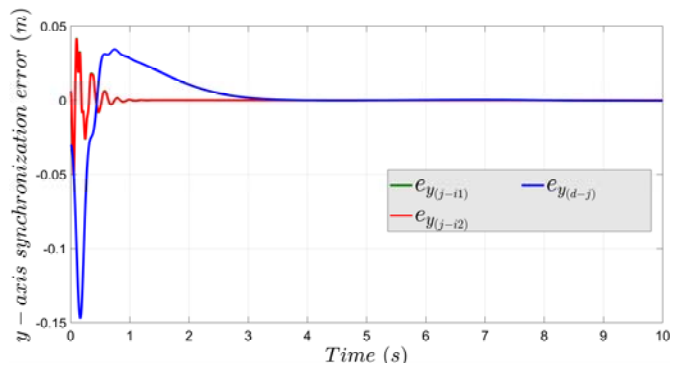


Fig. 4. Synchronization error on the y-axis of IM-Robot systems in the task space.

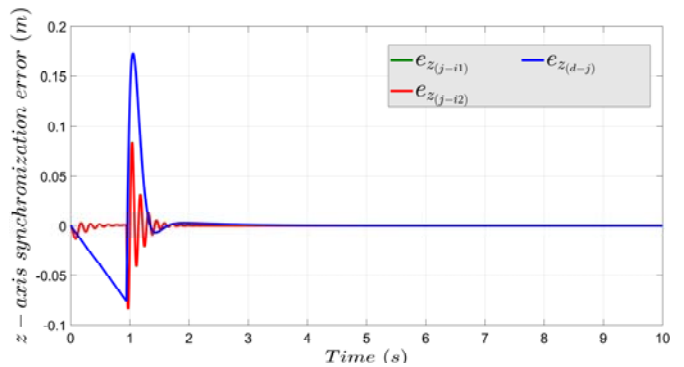


Fig. 5. Synchronization error on the z-axis of IM-Robot systems in the task space.

The Integral of Time Multiply Squared Error (ITSE) is given by:

$$ITSE_j = \int_{t_0}^{t_f} t (\chi_d - \chi_j)^2 dt \quad ITSE_i = \int_{t_0}^{t_f} t (\chi_j - \chi_i)^2 dt \quad (37)$$

The Integral of Time multiply Absolute Error (ITAE) is set as:

$$ITAE_j = \int_{t_0}^{t_f} t |\chi_d - \chi_j| dt \quad ITAE_i = \int_{t_0}^{t_f} t |\chi_j - \chi_i| dt \quad (38)$$

where $ITSE_j$ and $ITAE_j$ values the tracking error of the master IM-Robot system, the $ITSE_i$ and $ITAE_i$ are used for the synchronization error of the slave IM-Robots. The results of these indices are set in Table 3 and Table 4 where the values of the proposed synchronization approach are smaller in comparison with the others IM-Robot systems.

Table 3. ITSE results for tracking and synchronization

	Synchronization slave i_1 (m)	Synchronization slave i_2 (m)	Tracking Master j (m)
x	0.0188	0.0184	0.6178
y	0.0338	0.0328	1.6313
z	0.7628	0.7593	7.6836

Table 4. ITAE results for tracking and synchronization

	Synchronization slave i_1 (m)	Synchronization slave i_2 (m)	Tracking Master j (m)
x	2.3888	1.7075	32.7768
y	4.1840	2.9885	76.1635
z	21.3034	18.4092	83.4581

5. CONCLUSIONS

A synchronization control approach in the task space has been designed for whole systems IM-Robots (robot manipulators driven by induction motors), where the robot manipulator dynamics is combined with the induction motor dynamics to develop a control law based on Lyapunov formalism. Via simulations and considering the knowledge of the parameters, availability of the full state space and optimal sources, the proposed approach has shown synchronization errors hold asymptotically stable in the closed loop response.

Several works in the literature about synchronization have aimed in problematics like parametric uncertainty, only robot position availability, time delay and more. All of them consider ideal actuators; hence a special feature of this work is the inclusion of the induction motor dynamics and the robot dynamics in the synchronization scheme in the task space.

Fig. 6, Fig. 7 and Fig. 8 depict a zoom of synchronization errors of the slave IM-Robots in relation with x axis, y axis and z axis, respectively.

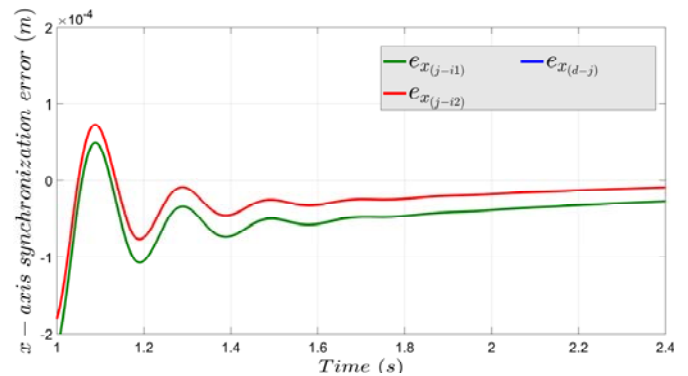


Fig. 6. Zoom of synchronization error on the x-axis of IM-Robot systems in the task space.

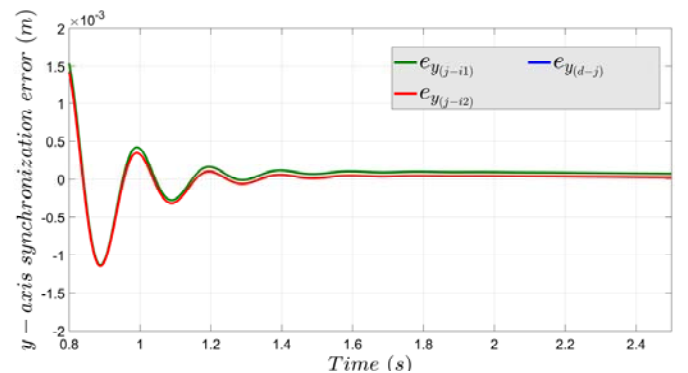


Fig. 7. Zoom of synchronization error on the y-axis of IM-Robot systems in the task space.

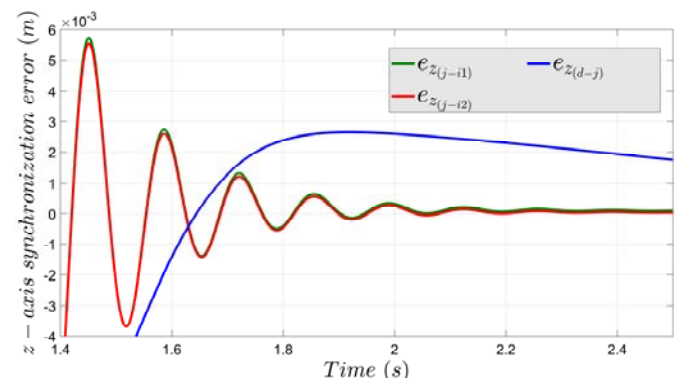


Fig. 8. Zoom of synchronization error on the z-axis of IM-Robot systems in the task space.

These figures show that the proposed synchronization approach provides a faster and more accurate convergence to zero compared to the other controller. Moreover, the performance indices $ITSE$ and $ITAE$ have been calculated to demonstrate the validity of this result. The further works will be directed on the implementation of the proposed synchronization approach to get experimental results.

REFERENCES

Abdessameud, A., Polushin, I., and Tayebi, A. (2013). Synchronization of Lagrangian Systems with Irregular

- Communication Delays. *IEEE Transactions on Automatic Control*, 59(1), 187-193.
- Aldana, C., Nuño, E., Basañez, L., and Romero, E. (2013). Operational Space Consensus of Multiple Heterogeneous Robots Without Velocity Measurements. *Journal of the Franklin Institute*, 351, 1517–1539.
- Anton, F., and Anton, S. (2011). Synchronizing robot motions in cooperative tasks. *Journal of Control Engineering and Applied Informatics*, 13(1), 43-48.
- Behal, A., Dixon, W., Dawson, D. M., and Xian, B. (2010). *Lyapunov-Based Control of Robotic Systems*. 372p. CRC Press. Florida, USA.
- Bondhus, A., Pettersen, K., and Nijmeijer, H. (2005). Master-Slave Synchronization of Robot Manipulators: Experimental Results. *IFAC Proceedings Volumes*, 38(1), 367-372.
- Bouteraa, Y., Ghommam, J., Poisson, G., and Derbel, N. (2011). Distributed Synchronization Control to Trajectory Tracking of Multiple Robot Manipulators. *Journal of Robotics*, 2011.
- Chung, S., and Slotine, J. (2009). Cooperative Robot Control and Concurrent Synchronization of Lagrangian Systems. *IEEE transactions on Robotics*, 25(3), 686-700.
- Cicek, E., Dasedemir, J., and Zergeroglu, E. (2014). Coordinated synchronization of multiple robot manipulators with dynamical uncertainty. *Transactions of the Institute of Measurement and Control*, 2014,1-12.
- Cicek, E., and Dasedemir, J. (2017). Output feedback synchronization of multiple robot systems under parametric uncertainties. *Transactions of the Institute of Measurement and Control*, 39(3), 277-287.
- De Diniz, E. C., Júnior, A. B., Honório, D. A., Barreto, L. H., and Dos Reis, L. L. (2012). An elbow planar manipulator driven by induction motors using sliding mode control for current loop. *Control and Cybernetics*, 41(2), 395-413.
- Duan, P., Duan, Z., and Wang, J. (2019). Task-space fully distributed tracking control of networked uncertain robotic manipulators without velocity measurements. *International Journal of Control*, 92(6), 1367-1380.
- Guerrero, G., and Tang, Y. (2001). Motion control of rigid robots driven by current-fed induction motors. *Mechatronics*, 11, 13-25.
- Hsu, S. H., and Fu, L. C. (2005). Adaptive decentralized control of robot manipulators driven by current-fed induction motors. *IEEE/ASME Transactions on Mechatronics*, 10(4), 465-468.
- Ihle, I. A. F., Arcak, M., and Fossen, T. I. (2007). Passivity-Based Designs for Synchronized Path Following. *Automatica*, 43(9), 1508-1518.
- Kyrkjebo, E., and Pettersen, K. (2008). Operational Space Synchronization of two Robot Manipulators Through a Virtual Velocity Estimate. *Modeling, Identification and Control*. 29(2), 59-66.
- Liu, Y., and Chopra, N. (2011). Controlled Synchronization of Heterogeneous Robotic Manipulators in the Task Space. *IEEE Transactions on Robotics*, 28(1), 268-275.
- Marino, R., Tomei, P., and Verrelli, C. (2010). *Induction Motor Control Design*. 350p. Springer. New York, USA.
- Min, H., Sun, F., Wang, S., and Li, H. (2009). Distributed adaptive consensus algorithm for networked Euler-Lagrange systems. *IET Control Theory and Applications*, 5(1), 145–154.
- Nuño, E., Ortega, R., Jayawardhana, B., and Basañez, L. (2013). Coordination of multi-agent Euler-Lagrange systems via energy-shaping: Networking improves robustness. *Automatica*, 49(10), 3065-3071.
- Rodriguez-Angeles, A. and Nijmeijer, H. (2004). Mutual Synchronization of Robots via Estimated State Feedback: A Cooperative Approach. *IEEE Transactions on Control Systems Technology*, 12(4), 542 – 554.
- Torres, F. J., Guerrero, G. V., Garcia, C. D., Gomez, J. F., Adam, M. and Escobar, R. F. (2016). Master-Slave Synchronization of Robots Manipulators Driven by Induction Motor. *IEEE Latin America Transactions*, 14(9), 3986 – 3991.
- Wang, H. (2013). Task-Space Synchronization of Networked Robotic Systems With Uncertain Kinematics and Dynamics. *IEEE Transactions on Automatic Control*, 58(12), 3169-3174.
- Yu, H., and Antsaklis, P. (2010). Passivity-Based Output Synchronization of Networked Euler-Lagrange Systems Subject to Nonholonomic Constraints. In *Proceedings of the 2010 American Control Conference*, 208-213. IEEE. Baltimore, USA.